Data in Brief 55 (2024) 110570

Contents lists available at ScienceDirect

Data in Brief

journal homepage: www.elsevier.com/locate/dib

Data Article

Tandem Mass Tag-10plex (TMT-10plex) phosphoproteomics dataset for comprehensive analysis of active compounds with tyrosine kinase inhibition activity

Yodying Yingchutrakul[a], Kiattawee Choowongkomon[b], Sucheewin Krobthong[c,*]

[a] National Center for Genetic Engineering and Biotechnology, NSTDA, Pathum Thani, 12120, Thailand
[b] Department of Biochemistry, Faculty of Science, Kasetsart University, Bangkok, 10900, Thailand
[c] Center of Excellence in Natural Products Chemistry (CENP), Department of Chemistry Faculty of Science, Chulalongkorn University, Bangkok 10330, Thailand

ARTICLE INFO

Article history:
Received 13 March 2024
Revised 22 May 2024
Accepted 24 May 2024
Available online 29 May 2024

Dataset link: TMT-10plex-based phosphoproteomics of bioactive compounds in A549 cells (Original data)

Keywords:
LC-MS/MS
Apoptosis
Lung epidermal cells
Isobaric mass tag
Post translational modification
Phosphorylation
EGFR

ABSTRACT

Bioactive compounds derived from natural products demonstrate a wide range of beneficial properties in cancer treatment. One popular approach to inhibiting cancer cell growth is by stimulating apoptosis. Interestingly, our research has discovered that traditional mushroom and isolated compounds from traditional herbs can induce apoptosis in A549 cells while inhibiting tyrosine kinase activities. We have identified two extracts from traditional mushrooms, *Phallus indusiatus* and *Fomes rimosus* (Berk.) *Cooke*, which exhibit promising abilities to activate apoptotic events in cells. Additionally, isolated compounds such as Chamuangone, Cannabigerol (CBG), Cannabidiol (CBD), and NP1-cyclic peptide have also demonstrated significant apoptotic activation capabilities. To further our understanding, we analyzed phosphoprotein changes in A549 cells exposed to these extracts and compounds, both with and without epidermal growth factor (EGF) stimulation. Our positive controls were two known drugs, Afatinib and Osimertinib, which are tyrosine kinase inhibitors with apoptotic stimulation abilities.

* Corresponding author at: Department of Chemistry, Faculty of Science, Chulalongkorn University, 254 Phaya Thai Rd, Wang Mai, Khet Pathum Wan, Bangkok 10330, Thailand.
E-mail address: sucheewin.k@chula.ac.th (S. Krobthong).

https://doi.org/10.1016/j.dib.2024.110570

In order to enrich our understanding of the kinase pathway, we conducted phosphoprotein enrichment analysis and identified altered phosphoproteins using LC-MS/MS. Across these testing conditions, we found that 1228 phosphoproteins were altered, providing valuable insights into the biochemical mechanisms underlying cell apoptosis in A549 cells through post-translational modifications of proteins. Furthermore, our findings not only shed light on the mechanisms of cell apoptosis in A549 cells but also offer promising avenues for future research and therapeutic development.

Specifications Table

Subject	*Proteomics*
Specific subject area	*TMT-based proteomics in cell lines*
Type of data	*Raw files, analyzed and processed files, Image, Table*
Data collection	*The data was acquired in data dependent mode by Orbitrap HF mass spectrometry coupled with Dionex Ultimate 3000 nano-RSLC high-performance liquid chromatography system.*
Data source location	*Institution: National Center for Genetic Engineering and Biotechnology, National Science and Technology Development Agency* *City/Town/Region: Pathumtani* *Country: Thailand*
Data accessibility	*Repository name: ProteomeXchange Consortium via the PRIDE* *Data identification number: PXD050555* *Direct URL to data:* https://www.ebi.ac.uk/pride/archive/projects/PXD050555

1. Value of the Data

- The high-resolution mass spectroscopy-based phosphoproteomic dataset holds significant value for research in the field of biochemistry. It provides the first comprehensive insight into the response of A549 cells to various compounds including Phallus indusiatus extract, Fomes rimosus (Berk.) Cooke extract, Chamuangone, CBG, CBD, and NP1-cyclic peptide.
- This valuable information facilitates the identification of protein biomarkers, which could play a crucial role in predicting disease progression and evaluating responses to bioactive compounds.
- Notably, this dataset marks the first phosphoproteome profiling encompassing two known cancer drugs, namely afatinib and Osimertinib. Researchers can utilize these data for comparative analyses with their own drug candidates, enhancing the efficacy of their experiments.
- These data serve as a resource for researchers seeking to identify specific protein biomarkers within the dataset. Furthermore, they aid in delineating potential pathways for enhancing diagnostic and therapeutic approaches, as well as in identifying targets for novel drug development.

2. Background

We conducted a comprehensive screening of bioactive compounds sourced from natural products, specifically targeting those capable of inducing apoptosis while inhibiting tyrosine kinase activity. Two extracts from traditional mushrooms, *Phallus indusiatus* and *Fomes rimosus* (Berk.) *Cooke*, exhibited promising abilities to activate apoptotic events in cells [1,2]. These extracts are linked to the inhibition of tyrosine kinase inhibitors (TKI) and the epidermal growth

Table 1
The sample code for isobaric tags with experimental condition.

Reporter Mass tag	Condition	Origin	Column name[1]
TMT-126	Afatinib	Pure compound	Reporter intensity corrected 1
TMT-127N	*Phallus indusiatus*	Extracts	Reporter intensity corrected 2
TMT-127C	Chamuangone	Pure compound	Reporter intensity corrected 3
TMT-128N	With epidermal growth factor (EGF)	–	Reporter intensity corrected 4
TMT-128C	CBG	Pure compound	Reporter intensity corrected 5
TMT-129N	CBD	Pure compound	Reporter intensity corrected 6
TMT-129C	*Fomes rimosus (Berk.) Cooke*	Extracts	Reporter intensity corrected 7
TMT-130N	Without EGF	–	Reporter intensity corrected 8
TMT-130C	NP1-cyclic peptide	Pure compound	Reporter intensity corrected 9
TMT-131	Osimertinib	Pure compound	Reporter intensity corrected 10

[1] It refers to the Excel file containing the phosphoproteomics results, named 'protein_abundance.xlsx'.

factor receptor (EGFR) pathways, both critical in cancer therapy. Additionally, isolated compounds such as Chamuangone, CBG, CBD, and NP1-cyclic peptide have demonstrated significant apoptotic activation capabilities [3-5]. These compounds can influence phosphorylated proteins by altering phosphorylation states within signaling pathways, potentially leading to the development of novel anti-cancer treatments targeting key regulatory proteins involved in cell growth and apoptosis. The integration of these natural extracts and compounds into therapeutic strategies highlights their potential in enhancing the efficacy of existing cancer therapies, particularly through the modulation of TKI and EGFR pathways. Our investigation encompassed a diverse range of compounds, including pure compounds and compound mixtures, all evaluated within the A549 cell line, which is an EGFR-positive human lung cancer cell line. To delve into the underlying molecular mechanisms, we employed phosphoproteomics analysis, which enabled us to comprehensively assess the impact of these bioactive compounds on cellular pathways. Through labeling digested proteins with distinct isobaric tags, we meticulously examined the cellular response to each compound. In our experimental design, we included two established chemical drugs, Afatinib and Osimertinib, serving as positive controls. These drugs, both kinase inhibitors utilized in cancer treatment, operate via distinct mechanisms and target different kinases. By comparing the effects of our test compounds with these controls, we aimed to elucidate their potential therapeutic relevance and mechanisms of action. Among the compounds examined were extracts from *Phallus indusiatus* and *Fomes rimosus (Berk.) Cooke*, as well as specific compounds like Chamuangone [6], CBG, CBD, and NP1-cyclic peptide [5]. The A549 cell line was chosen to model the study of TKI due to its relevance in non-small cell lung cancer (NSCLC) research. A549 cells are derived from a human lung adenocarcinoma, making them a representative model for NSCLC. They have been extensively used to study the effects of various tyrosine kinase inhibitors on apoptosis events. Our investigation encompassed evaluations of these extracts and compounds in the A549 cells, providing insights into their efficacy and potential interactions with growth factor signaling pathways.

3. Data Description

In this dataset, a total of ten experimental conditions were examined using TMT-based phosphoproteomics. These conditions included treatments with various compounds and extracts: *Phallus indusiatus* extract, *Fomes rimosus* (Berk.) *Cooke* extract, Chamuangone, CBG, CBD, NP1-cyclic peptide, Afatinib, and Osimertinib. Each of these compounds was investigated under two overarching cellular environments—one stimulated with EGF and the other without EGF stimulation (plain cells for control condition). Our samples were labelled using different TMT tags as shown in Table 1.

The instrument and sample processing were validated to ensure the reliability of the dataset. Consequently, the base peak chromatogram (BPC) of four fractions of phosphopeptides

Table 2
Elution information of phosphorylated peptides that passed through High pH Reversed-Phase fractionation, along with the corresponding LC-MS/MS file names correlated with each fraction.

Fraction No.	Acetonitrile (µL)	0.1 % Triethylamine (µL)	%acetonitrile	File name (.raw)
1	50	950	5	F1_1.raw, F1_2.raw, and F1_3.raw
2	100	900	10	F2_1.raw, F2_2.raw, and F2_3.raw
3	220	780	22	F3_1.raw, F3_2.raw, and F3_3.raw
4	60	40	60	F4_1.raw, F4_2.raw, and F4_3.raw

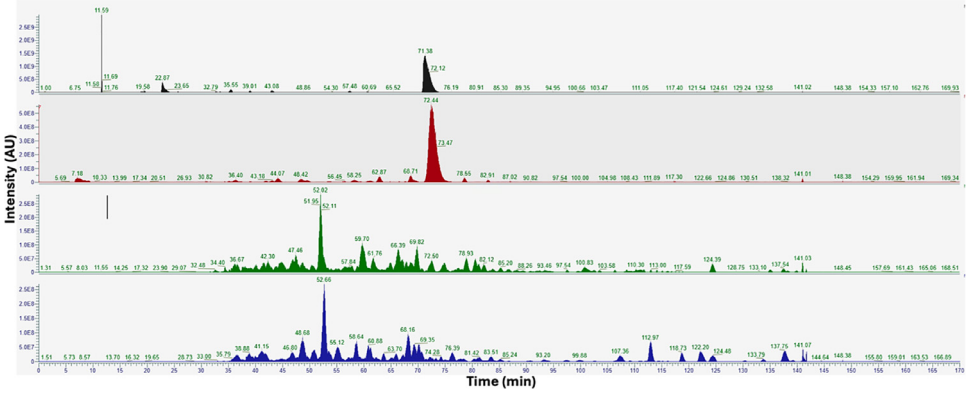

Fig. 1. BPC of phosphopeptides. The x-axis represents retention time, while the y-axis indicates intensity. Chromatograms for the 5 %, 10 %, 22 %, and 60 % acetonitrile fractions are depicted in black, red, green, and blue, respectively. (For interpretation of the references to color in this figure legend, the reader is referred to the web version of this article.)

(as outlined in Table 2) is presented in Fig. 1. Notably, the BPC across various fractions exhibits distinct profiles. Specifically, the mass spectra within the 22 % and 60 % acetonitrile fractions exhibited higher peak intensities compared to those in the 5 % and 10 % acetonitrile fractions.

Phosphoproteomic data were acquired using LC-MS/MS, resulting in a total of 1329 proteins from 4 fractions and 3 technical replicates for each group (12 samples in total). To ensure the reliability of the results, proteins containing only one peptide were excluded. The protein intensities for each condition are listed in the 'Reporter intensity corrected' column of the 'protein_abundance.xlsx' file. The correlations between experimental conditions and protein intensity of the Excel file are presented in Table 1. Please refer to the Excel file for the identified proteins and their corresponding gene names, which are listed in the 'protein names' and 'gene names' columns, respectively. Additionally, the file includes information on the number of identified peptides, unique peptides, and *q*-value.

PCA on phosphoproteomic data was successfully done. The two principal components (PC1 and PC2) were used to visualize the data, providing insights into the clustering and separation of samples based on their phosphoproteomic profiles (Fig. 2). The PCA revealed that PC1 explains approximately 96.32 % of the variance and the PC2 explains approximately 1.38 % of the variance. Together, the first two principal components account for approximately 97.7 % of the total variance in the dataset. This high percentage of variance explained by the combined PC1 and PC2 suggests that the experimental groups are mostly differentiated along the x-axis in the PCA space.

Given the inclusion of two positive control drugs in the experiments, the PCA analysis offers valuable insights as a preliminary guideline for understanding the response of phosphoproteins. Specifically, phosphoproteins responding to CBD and CBG exhibited a closer association with Osimertinib than with Afatinib, as highlighted in the purple region of Fig. 1. Conversely, phosphoproteins associated with *Phallus indusiatus* extract, *Fomes rimosus (Berk.) Cooke* extract,

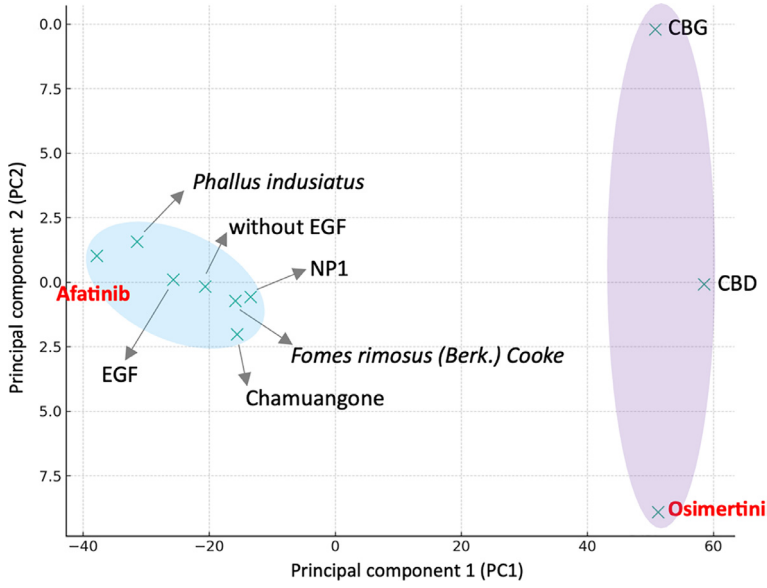

Fig. 2. PCA of phosphoproteomics data across experimental groups. This plot visualizes the distribution of 10 experimental groups, including negative control (EGF and without EGF), positive control (Afatinib and Osimertinib) and treated samples. The plot delineates the clustering of samples, with specific regions highlighted to indicate similarities in phosphoprotein expression profiles: the purple region suggests a closer relationship between phosphoproteins responding to CBD and CBG with Osimertinib, while the blue region indicates a greater similarity of phosphoproteins associated with *Phallus indusiatus extract, Fomes rimosus (Berk.) Cooke extract*, Chamuangone, and NP1 peptide to Afatinib. (For interpretation of the references to color in this figure legend, the reader is referred to the web version of this article.)

Chamuangone, and NP1 peptide showed a greater proximity to Afatinib than to Osimertinib, depicted in the blue region of the same figure. This differential clustering provides a basis for further exploration into the specific interactions and pathways influenced by these conditions.

The relative phosphoprotein abundance from all experimental group were aligned together and clustered using the Self Organizing Tree Algorithm (SOTA) to get a holistic view of the phosphoproteome profiling across all experimental groups (Fig. 3). After clustering, eleven distinct clusters were constructed based on the phosphoprotein profiling.

The columns in the SOTA dendrogram represent the relative abundance of phosphoproteins across 10 experimental groups. Each column corresponds to an experimental testing code as indicated in Table 1. The rows depict the average abundance level of proteins within each cluster. Red indicates higher abundance levels, while green indicates lower abundance levels. The analysis unveiled that Cluster ID eleven (highlighted in red) exhibits the highest cluster diversity (2.20), encompassing 25 proteins.

4. Experimental Design, Materials and Methods

4.1. Experimental design, treatment condition, and sample coding correlation

The effect of bioactive compounds on A549 cells was explored through a phosphoproteomics approach. Before setting up the experiment, the A549 cells were maintained at 37 °C in a humidified incubator with a 5 % CO_2 environment in Dulbecco's Modified Eagle's Medium with l-glutamine, supplemented with 10 % fetal calf serum (FBS), 1 × non-essential amino acids, 1 mM sodium pyruvate, and antibiotics (100 µg/mL penicillin and 10 µg/mL streptomycin) (Gibco, USA). The medium was replenished every 3 days for 3 cycles. After that, A549 cells were treated with

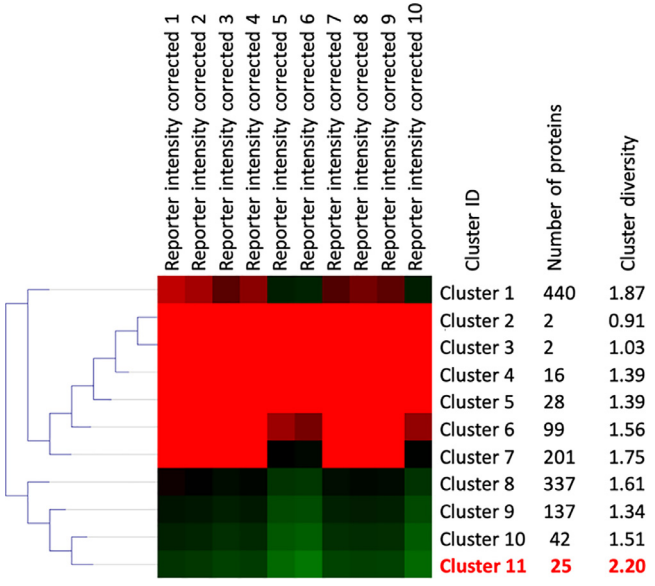

Fig. 3. SOTA of phosphoprotein abundance by experimental sample. The heat-map shows the similarity of protein abundance in each experimental sample group. The differential phosphoprotein abundance was grouped into 11 clusters with different phosphoprotein profiles using centroid distance. Color key expression: green and red represent the lower and higher differential changes. (For interpretation of the references to color in this figure legend, the reader is referred to the web version of this article.)

fresh medium containing 0.1 % FBS. The concentration of all extracts and compounds in this experiment was fixed at 10 µg/mL for the *Phallus indusiatus* extract and *Fomes rimosus* (Berk.) *Cooke* extract, and 10 µM for Chamuangone, CBG, CBD, NP1-cyclic peptide, Afatinib, and Osimertinib, respectively. After 24 h of incubation, the cells were harvested for protein extraction. We had one condition with EGF stimulation to validate tyrosine kinase activation. The condition without EGF was used as the plain cells or control condition for this experiment. We employed isobaric mass tags, TMT^{TM} 10 plex, to label the different 10 experimental groups. These labelled samples were pooled into a single reaction, fractionated, and analyzed simultaneously. The conditions and intensities of the isobaric mass tags within each experimental group are detailed in Table 1.

4.2. Protein extraction, cleaning-up and digestion

A549 cells in various conditions were lysed using a lysis buffer solution, comprising 0.5 % TritonX-100, 2 mM TCEP, 50 mM HEPES-KOH (pH 8.2), and supplemented with a protease and phosphatase inhibitor cocktail. The lysed tissue was subjected to sonication at 80 % amplitude, alternating 3 s on and 7 s off for a total of three cycles (30 s in total). The protein solution was collected by centrifugation at 14,000 *g* for 20 min at 12 °C. The protein concentrations were determined by the bicinchoninic acid assay kit (Pierce, New York, NY, USA), using bovine serum albumin as the standard. For phosphoprotein enrichment analysis, we used 3 mg. at concentration of 5 µg/µL for the enrichment. The phosphoprotein enrichment was conducted by Pierce® Phosphoprotein Enrichment Kit (Thermo Fisher Scientific, USA). Subsequently, the protein concentration was adjusted to 1 µg/µL by diluting the protein solution with the binding/washing reagent to achieve a final concentration of 1 µg/µL, following the instructions provided in the kit. The elution of phosphoproteins was carried out using size-exclusion chromatography with Zeba^{TM} Spin Desalting Columns (Thermo Fisher Scientific, USA). Following elution, the protein concentration of the flow-through fraction was measured and adjusted to 0.6 µg/µL.

A total of 60 µg protein was subjected to gel-free based digestion using previous protocol with minor modification [7]. Briefly, the protein solution was precipitated using ice-cold acetone at 1:10 (v/v) ratio at −20 °C for 16 h. Then, the samples were subjected to centrifugation at 16,000 *g* for 15 min and the supernatants were discarded. The protein pellet was reconstituted in 0.25 % RapiGest SF (Waters, UK) in 10 mM HEPES-KOH, pH 8.2 and 5 mM NaCl. For the protein digestion and clean-up, the protein amount of 30 µg was subjected to gel-free-based digestion method. Reduction of the sulfhydryl bonds by using 2 mM TCEP in 10 mM HEPES-KOH, pH 8.2 at 60 °C for 1 hour and alkylation of sulfhydryl by 10 mM IAA in 10 mM HEPES-KOH, pH 8.2 at room temperature for 40 min in the dark. The solution was cleaned up by the Zeba™ Spin Desalting Columns (Thermo Fisher Scientific, USA). The flow-through solution was enzymatically digested by trypsin (Promega, Germany) at a ratio of 1:50 (enzyme: protein) and incubated at 38 °C for 3 h. The reaction was terminated by incubation at 90 °C for 15 min. The supernatant was collected by centrifugation at 16,000 g for 20 min. The tryptic peptides were dried and reconstituted in 25 µL of 100 mM HEPES-KOH, pH 8.2 prior to labeling. Peptide concentration is measured using peptide quantification kit (Pierce™ Quantitative Peptide Assays & Standards). The experiment was conducted in three independent experiments ($n = 3$). For TMT labeling (after reconstituting each tube with 41 µL of acetonitrile), all of phosphorylated peptides from each sample were labeled using TMT10plex™ Label reagent set (Lot:XE342654) reaction for 1 hour at room temperature. The sample group of the experiment was already shown in Table 1. The reaction was quenched using 5 % hydroxylamine for 15 min at room temperature. All labeled samples were combined into a single tube, dried, reconstituted in 1 % TFA, and underwent desalting and clean-up using the Pierce™ High pH Reversed-Phase Peptide Fractionation Kit (Thermo Fisher Scientific, USA). The phosphorylated peptides underwent fractionation into four fractions utilizing acetonitrile and triethylamine at a volume of 350 µL per fraction. Detailed information regarding the fractionations, including corresponding file names in the raw data, is presented in Table 2.

All fractions were dried by speed-vacuum, reconstituted in 0.1 % formic acid, and transferred to a TruView LCMS vial (Waters, UK). Each fractionation was injected independently in triplicate for technical replication.

4.3. LC-MS/MS setting for TMT-based proteomics analysis

The LC-MS/MS spectrum data were collected in the positive mode with an HF Hybrid Quadrupole-Orbitrap™ Mass Spectrometer combined with nano-LC system equipped with an EasySpray C18 column (Thermo Scientific™ ES903; 75 µm × 50 cm, 2.0 µm) using previous protocol with minor modifications [7]. Briefly, mobile phase A consisted of 0.1 % formic acid in water and mobile phase B consisted of 95 % acetonitrile with 0.1 % formic acid. Separation was conducted with a linear gradient of 5 %–50 % mobile phase B at a constant flow rate of 300 nL/min over a period of 175 min. The TMT-labelled tryptic peptides were analyzed by applying a data-dependent acquisition method, followed by a higher-energy collisional dissociation (HCD). Normalized collision energy by HCD was set at 32. Full scan mass spectra were acquired at an *m/z* ratio of 400 to 1500 with an AGC target set at 3×10^6 ions, a resolution of 120k, and injection time was 60 ms. MS/MS scanning was initiated when the automatic gain control target reached $3e^6$ ions and, a resolution of 60k, and injection time was 100 ms. Isolation windows was 1.4 *m/z*. The mass spectrometry proteomics data have been deposited to the ProteomeXchange Consortium via the PRIDE partner repository with the dataset identifier PXD050555 [8].

4.4. Data analysis for TMT-based proteomics analysis

Raw files from all fractions ($n = 12$) were analyzed using Maxquant (version 2.0.11) [6]. The reporter ion (MS2) was The peptides quantification is performed by measuring the intensities of fragment reporter ions (TMT^{126} – TMT^{131}) using default setting. The reporter ion isotopic distribution was corrected follow Table 3.

Table 3
TMT-reporter ion correction value. The correction values indicating the percentages of each reporter ion that have masses differing by the nominal reporter ion mass.

Reporter Mass tag	Mass of reporter ion (Da)	Reporter ion isotopic distribution (%)				
		−2	−1	Mono. mass	+1	+2
TMT-126	127.127726	-	-	-	7.4	-
TMT-127N	127.124761	-	0.1	-	7.8	0.1
TMT-127C	127.131081	-	0.8	-	6.9	0.1
TMT-128N	128.128116	-	1.2	-	6.3	-
TMT-128C	128.134436	-	1.3	-	5.7	0.1
TMT-129N	129.131471	-	1.5	-	5.7	0.1
TMT-129C	129.137790	0.3	2.7	-	4.8	-
TMT-130N	130.134825	-	2.2	-	4.6	-
TMT-130C	130.141145	-	3.1	-	3.6	-
TMT-131	131.138180	0.1	2.9		3.8	-

The mass spectra were searched against the Human database (reviewed UniProtK; 20,434 sequences; retrieved on January 15, 2024) using the following criteria: strict trypsin specificity, allowing up to two missed cleavages, a fixed carbamidomethyl modification on cysteine (+57.0215 Da), TMT tags on the peptide N-terminus and lysine, with methionine oxidation (+15.9949 Da), and N-terminal acetylation (+42.0106 Da) as variable modifications. The search parameters included a precursor ion tolerance of 20 ppm. A 1 % false discovery rate threshold was applied at the protein level. All other MaxQuant settings were kept at default [2]. For post-processing analysis, phosphoprotein expression data were adjusted by adding "1" to all matrix data and then transformed into Log2 values. PCA was performed using the scikit-learn library, a widely-used machine learning library in Python. Specifically, the PCA implementation from the decomposition module of scikit-learn was utilized [9]. The heatmap depicting phosphoprotein abundance was generated using the MultiExperiment Viewer (MeV) for SOTA clustering based on the expression data, following previously reported methods without any modifications [10].

Limitations

Our analysis could not be conducted for bio-replication analysis due to the substantial amount of protein samples. Following phosphoprotein enrichment experiments, we successfully recovered approximately 4 % of phosphoproteins from the whole proteins.

Ethics Statement

The current work does not involve human subjects, animal experiments, or any data collected from social media platforms.

Data Availability

TMT-10plex-based phosphoproteomics of bioactive compounds in A549 cells (Original data) (ProteomeXchange Consortium via the PRIDE).

CRediT Author Statement

Yodying Yingchutrakul: Data curation, Formal analysis, Investigation, Methodology, Software, Visualization, Writing – original draft, Writing – review & editing; **Kiattawee Choowongkomon:** Conceptualization, Funding acquisition, Project administration, Writing – review & editing;

Sucheewin Krobthong: Conceptualization, Funding acquisition, Methodology, Project administration, Resources, Supervision, Writing – review & editing.

Acknowledgements

This research did not receive any specific grant from funding agencies in the public, commercial, or not-for-profit sectors.

Declaration of Competing Interest

The authors declare that they have no known competing financial interests or personal relationships that could have appeared to influence the work reported in this paper.

Supplementary Materials

Supplementary material associated with this article can be found, in the online version, at doi:10.1016/j.dib.2024.110570.

References

[1] W. Liao, et al., Preparation and characterization of dictyophora indusiata polysaccharide-zinc complex and its augmented antiproliferative activity on human cancer cells, J. Agric. Food Chem. 63 (29) (2015) 6525–6534.
[2] Q. Xue, et al., Immunostimulatory and anti-tumor activity of a water-soluble polysaccharide from Phellinus baumii mycelia, World J. Microbiol. Biotechnol. 27 (5) (2011) 1017–1023.
[3] P. Sae-Lim, et al., Chamuangone from Garcinia cowa leaves inhibits cell proliferation and migration and induces cell apoptosis in human cervical cancer in vitro, J. Pharm. Pharmacol. 72 (3) (2020) 470–480.
[4] Z. Fu, et al., Cannabidiol regulates apoptosis and autophagy in inflammation and cancer: a review, Front. Pharmacol. 14 (2023) 1094020.
[5] N. Jiwacharoenchai, et al., A novel cyclic NP1 reveals obstruction of EGFR kinase activity and attenuation of EGFR–driven cell lines, J. Cell Biochem. 123 (2) (2022) 248–258.
[6] S. Tyanova, T. Temu, J. Cox, The MaxQuant computational platform for mass spectrometry-based shotgun proteomics, Nat. Protoc. 11 (12) (2016) 2301–2319.
[7] S. Krobthong, et al., Utilizing quantitative proteomics to identify species-specific protein therapeutic targets for the treatment of leishmaniasis, ACS Omega 7 (15) (2022) 12580–12588.
[8] Y. Perez-Riverol, et al., The PRIDE database resources in 2022: a hub for mass spectrometry-based proteomics evidences, Nucleic Acids Res. 50 (D1) (2022) D543–D552.
[9] T. Tanaka, [[Fundamentals] 5. Python+scikit-learn for machine learning in medical imaging], Nihon Hoshasen Gijutsu Gakkai Zasshi 79 (10) (2023) 1189–1193.
[10] S. Krobthong, et al., Evaluation of potential anti-metastatic and antioxidative abilities of natural peptides derived from Tecoma stans (L.) Juss. ex Kunth in A549 cells, PeerJ 10 (2022) e13693.